The Generalized Fundamental Diagram of Traffic and Possible Applications

Elad Tomer[1], Leonid A. Safonov[1,2], and Shlomo Havlin[1]

[1] Minerva Center and Department of Physics,
Bar-Ilan University, 52900 Ramat-Gan, Israel
[2] Department of Applied Mathematics and Mechanics,
Voronezh State University, 394693 Voronezh, Russia

Abstract. We propose a new optimization strategy based on inducing stop-and-go waves on the main road and controlling their wavelength. Using numerical simulations of a recent stochastic car-following model [E. Tomer, L. Safonov, S. Havlin: Phys. Rev. Lett. **84**, 382 (2000)] we show that this strategy yields optimization of traffic flow in systems with a localized periodic inhomogeneity, such as signalized intersections and entry ramps. The optimization process is explained by our finding of a generalized fundamental diagram (GFD) for traffic, namely a flux-density-wavelength relation. Projecting the GFD on the density-flux plane yields a two-dimensional region of stable states, qualitatively similar to that found empirically [B.S Kerner: Phys. Rev. Lett. **81**, 3797 (1998)] in synchronized traffic. The empirical finding of the dependence of the wavelength on the average velocity can also be explained using the same approach.

1 Introduction

Traffic flow has been a subject of comprehensive study for more than half a century, [1–26] due to its theoretical and practical importance. Recently this field has attracted much interest, especially after new empirical and theoretical studies have shown its clear relation to physical phenomena of current interest, such as phase transitions, critical phenomena, nonlinear dynamics, and chaos (for reviews see e.g. [1–3]).

One of the main open questions in this field regards the validity of the basic concept of the 'fundamental diagram' [4–6] – a functional relation between the flux and the density of cars. This generally recognized relation, used in almost every study in this field, was challenged recently by empirical findings of Kerner [7,8] indicating that such a fundamental diagram does not exist. Instead, stable synchronized traffic states display a two-dimensional region in the density-flux plane. Consequently, the wide scattering of data points representing congested traffic cannot be attributed only to measurement fluctuations, but also to the existence of a range of stable flux values for a given density. The existence of a range of flux values gives rise to a possibility of manipulating the system in order to achieve the highest possible flux.

Other empirical observations show that traffic flow demonstrates complex physical phenomena, both on macroscopic and microscopic scales. Among these experimental findings are: (i) The existence of three phases in traffic flow [9]:

Free flow, Synchronized flow, and traffic jams; (ii) Metastable free flow in some intermediate range of densities, and hysteresis in transitions between free and synchronized flow [9]; (iii) Periodic wave motion in stop-and-go traffic, characterized by a typical time period (see [10]), and a 'wavelength' (distance between two nearest narrow jams) [7]. The wavelength is an increasing function of the average velocity [7] for the intermediate range of velocities.

Recently, a stochastic inertial car-following model that may explain (i)-(ii) and other empirical results was proposed [11,12]. The deterministic version of the model shows transitions between three phases with increasing the density: homogeneous free flow, stop-and-go waves, and congested homogeneous flow. Free flow is metastable for some range of densities, leading to hysteresis in the transitions to congested traffic. Moreover, multiple inhomogeneous congested traffic states coexist in the intermediate regime [11]. These stop-and-go waves are periodic for homogeneous systems with periodic boundary conditions, and differ in their wavelength. These states correspond to limit cycles in the phase space. They can be found analitically near the bifurcation points, and can be traced numerically far from this point [12]. Transitions between these states can be induced by noise.

Earlier studies of microscopic car-following models, such as the optimal velocity model (OVM) [13], also report on stable congested states corresponding to limit cycles in phase space. These limit cycles were found to be universal objects [14]. In this model, as well as in other microscopic models such as the Nagel-Schreckenerg (NS) cellular-automata model [15], the flux f does not depend on the exact configuration of the congested state, and f is a function only of the density ρ. In general, traffic flow models predict (or assume) a single-value or double-value function $f(\rho)$ – namely a fundamental diagram – unlike the explerimental findings of a $2D$ region in the density-flux plane mentioned above.

In this paper we propose a possible explanation to the experimental findings showing that such fundamental diagram does not exist. Studying the deterministic version of our model [11] we find a $2D$ region in the density-flux plane that is caused by the existence of a hidden parameter, namely, the wavelength of the stop-and-go states. Therefore, the fundamental diagram $f(\rho)$ has to be generalized to a density-wavelength-flux relation. We call this relation the *generalized fundamental diagram* (GFD) of traffic. We further analyze the stability of the stop-and-go states, and show that the noise stability threshold is a function of the wavelength – a function which has a single maximum. The wavelength of this most stable state is an increasing function of the average velocity for the intermediate range of velocities – qualitatively similar to that found experimentally, see (iii) above.

Finally, we propose a novel optimization strategy, which aims to optimize traffic by approaching the highest flux values in this $2D$ region. Our approach is based on inducing stable stop-and-go waves on the main road and controlling their wavelength. It is shown that this strategy yields optimization of traffic flow when implemented in systems with a localized periodic inhomogeneity, such as

signalized intersections and entry ramps, in cases of over-saturation. The promising numerical results for optimization are not predicted by common theories. We explain the optimization process using our finding of a GFD, together with the finding of the existence of noise stability threshold mentioned above. If approved by field experiments, this method would enable to make use of the existing infrastructure to further optimize congested traffic, especially for high densities were congestion cannot be relieved.

The paper is organized as follows. The car-following model is presented in Sec. 2, where the relation to NS-type models is also discussed. In Sec. 3 the GFD is derived and a $2D$ region in the density-flux plane is found. Sec. 4 discusses the influence of noise, and a qualitative agreement with the experimental findings (iii) above is shown in Sec. 5. The new theoretical results are then applied to propose a novel optimization method in Sec. 6.

2 The Model

In microscopic traffic models approach [11–23], traffic is treated as a flow of interacting particles. In particular, car-following models [11–14,19–22] are usually defined by a set of ordinary differential equations, each of them describing the motion of a single car. In inertial car-following models, these equations, which are usually of second order, describe the interaction between following cars. This interaction is defined by a relation between the acceleration a_n of the n'th car, its headway Δx_n, velocity v_n, and velocity difference with the car ahead Δv_n, i.e., $a_n = a(\Delta x_n, v_n, \Delta v_n)$. Newton's third law is not satisfied for these type of interactions, since a leading car affects its follower, but not vice versa.

We assume [11] that the acceleration of each car is determined by four factors:

(a) desire to maintain a safety time gap from the car ahead,
(b) pre-braking if the car ahead is much slower,
(c) desire not to exceed significantly the speed limit,
(d) random noise.

These four assumptions are represented by four corresponding terms in the equations of motion,

$$a_n = a_{(1)}(\Delta x_n, v_n) + a_{(2)}(\Delta v_n, \Delta x_n) + a_{(3)}(v_n) + \eta'. \tag{1}$$

In the following we derive each term in a simple way that still maintain the essential characteristics of human driving described by assumptions (a)-(d). We first consider a single lane homogeneous system with periodic boundary conditions, length L, having N vehicles. It is assumed that all drivers have the same parameters (identical drivers). Initial conditions can be homogeneous, random, or periodic.

(a) Maitaining safety time gap: To define the first term in the equation of motion (1), $a_{(1)}(\Delta x_n, v_n)$, let us assume that all drivers wish to maintain a safety time gap T from the car ahead when driving in a platoon. This time

gap T is an estimation of the maximal response time of a driver. A time gap of approximately $T = 2s$ is usually recommanded for safe driving. Maintaining this time gap, a driver can react safely even to sharp braking of the car ahead, since that by the end of this time T he starts braking when he is at the same position as was the car ahead when it started braking. Thus, the optimal headway is

$$\Delta x_n^0 = v_n T + D, \tag{2}$$

where D is the minimal distance between consecutive cars (car length plus bumper to bumper distance).

Following the above considerations, we can now define $a_{(1)}(\Delta x_n)$. A realistic relation between acceleration and headway should have the following characteristics:

(i) Zero acceleration for the optimal headway: $a_{(1)}(\Delta x_n = \Delta x_n^0) = 0$.
(ii) Small of headway yield sharp braking: for $\Delta x_n \ll \Delta x_n^0$, $a_{(1)}(\Delta x_n) \to -\infty$.
(iii) $a_{(1)}$ is an increasing function of Δx_n.

The simplest choice of $a_{(1)}(\Delta x_n)$ that satisfies (i)-(iii) is

$$a_{(1)} = A\left(1 - \frac{\Delta x_n^0}{\Delta x_n}\right), \tag{3}$$

where A is a sensitivity parameter (aggressive drivers can be represented by relatively high values of A). In contrast to the optimal velocity model [13], where the acceleration depends on the difference between v_n and an optimal velocity $v_0(\Delta x_n)$, here the acceleration depends on the difference between Δx_n and the optimal headway $\Delta x_n^0(v_n)$. The explicit dependence on the headway Δx_n enable us to make the model free of frequent collisions for every choice of parameters values (see also [20,13]).

As a matter of fact, other possible choices of $a_{(1)}$ that satisfies (i)-(iii) can also be defined. To find out how our results are affected by the choice of $a_{(1)}$ we also consider a simple logarithmic relation,

$$a_{(1)} = Alog\left(\frac{\Delta x_n}{\Delta x_n^0}\right). \tag{4}$$

The functions $a_{(1)}(\Delta x_n)$ given by Eqs. (3)-(4) are plotted in Fig. 1a. The qualitative (and sometimes even quantitative) characteristics of the stable states of the model are independent of the exact functional choice of $a_{(1)}$. In both cases the solutions are fixed points (homogeneous flow) and limit cycles (stop-and-go waves). The range of density values for which homogeneous solution is stable is exactly the same in both cases. This is because the slope $a'_{(1)}(\Delta x_n^0)$ is the only important property of this function for determining this stability range (see [11]), and it is equal to A for both choices of $a_{(1)}$. In addition, our finding of the generalized fundamental diagram (Sec. 3) is valid for both choices. Therefore it can be assumed that the results presented below are independent on the exact choice of

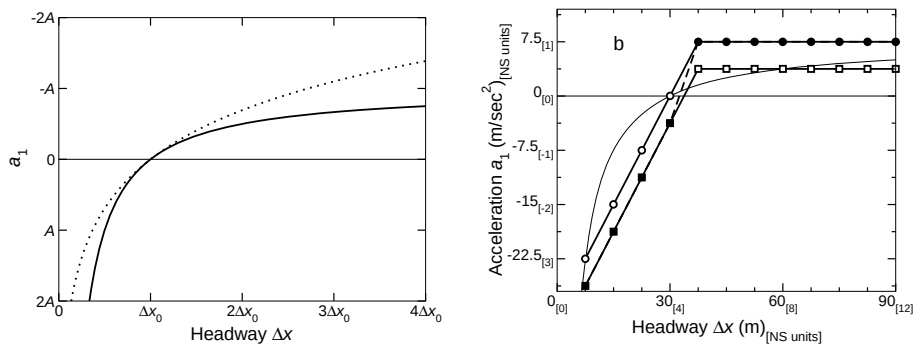

Fig. 1. a. A plot of the function $a_{(1)}(\Delta x_n)$ given by Eq. (3) (solid curve), and of the that given by the logarithmic expression, Eq. (4), (dotted curve). **b**. The relation between acceleration and headway $a_{(1)}(\Delta x_n)$ for the deterministic NS model with $v_{max} = 5$ and $v_n = 3$ (circles), for the stochastic NS model with the same parameters and $p = 0.5$ (squares), for the NP model with the same parameters (full symbols, dashed curve), and for our model, Eq. (3), with the corresponding parameters (thin curve).

$a_{(1)}$ that satisfies conditions (i)-(iii). In the following we use the function given by Eq. (3).

(b) Pre-braking: The first term $a_{(1)}$ in Eq. (1) might be sufficient when cars move in a platoon, so that following cars have approximately the same speed. But when a fast car is approaching a much slower car, i.e. $\Delta v_n < 0$ and $|\Delta v_n| \sim v_{n+1}$, this term is not enough (see below). Thus it is necessary to introduce a second term, $a_{(2)}(\Delta v_n)$, in the equation of motion. This term represents the additional negative acceleration caused by this negative velocities difference. If such a term is not included, a fast car approaching a standing car, for example, would start braking only at about time T before crashing into it – which is, of course, unrealistic.

To determine this term, let us define x'_n and v'_n as the position and velocity of the n'th car in the system of coordinates of the $n+1$'th car. Clearly $x'_n = -\Delta x_n$, and $v'_n = -\Delta v_n$. We discuss here the case of $v'_n > 0$, and try to estimate the negative acceleration $a_{(2)}$ required to reduce v'_n to zero while car n is approaching the slower $n+1$ car, i.e. x'_n is reduced to the minimal headway D. Assuming that this acceleration $a_{(2)}$ is constant, the time of this process is $t = \Delta v_n / a_{(2)}$. Substituting t in $-D = -\Delta x_n - \Delta v_n t + \frac{1}{2} a_{(2)} t^2$, one obtains

$$a_{(2)} = -\frac{(\Delta v_n)^2}{2(\Delta x_n - D)}, \quad \Delta v_n < 0. \tag{5}$$

(c) Speed limit: As in real driving, a car in our model can exceed the speed limit. Therefore we denote this speed limit v_{per} ('permitted velocity'). The corresponding dissipative third term in Eq. (1), $a_{(3)}$, represents the effective 'repulsive force' acting when the velocity exceeds the permitted velocity. The

simplest choice of this a term is

$$a_{(3)} = -k(v_n - v_{per}), \quad v_n > v_{per}, \tag{6}$$

where k is a constant, representing the coupling to the permitted velocity (relatively high values of k represent higher 'obedience' to this speed limit).

(d) Randomness: The randomness in the driver behavior is usually represented by white uncorrelated noise, denoted by $\eta'(x,t)$ in Eq. (1). For numerical realization of this type of noise, uniformly distributed random numbers are chosen for each car at every iteration. In the following we denote by η the amplitude of this distribution. According to the central limit theorem, the noise becomes Gaussian as the numerical time interval Δt satisfies $\Delta t \ll T$. In this case the effective amplitude of the noise is proportional to $\eta\sqrt{\Delta t}$.

We can therefore derive a system of equations representing the motion in this model,

$$a_n = A\left(1 - \frac{\Delta x_n^0}{\Delta x_n}\right) - \frac{Z^2(-\Delta v_n)}{2(\Delta x_n - D)} - kZ(v_n - v_{per}) + \eta', \tag{7}$$

where the function Z(x) is defined as $Z(x) = (x + |x|)/2$. In the following we use this version of the model with parallel updating rule and white noise, unless else is mentioned. The numerical solutions presented below are plotted for the parameters values $T = 2(s)$, $D = 5(m)$, $A = 3(m/s^2)$ $v_{per} = 25(m/s)$, $k = 2(s^{-1})$, and a numerical time interval $\Delta t = 0.1sec$.

To compare the Nagel-Schreckenberg (NS) model [15] with our model, let us determine $a_{(1)}(\Delta x_n, v_n)$ and $a_{(3)}(v_n)$ for the deterministic NS model [16]. Since the speed limit v_{per} in the NS model is really a maximal velocity, it corresponds to Eq. (6) with the limit $k \to \infty$. To find the corresponding $a_{(1)}$ of the NS model, we should first define an optimal headway for the NS model. This optimal headway is $\Delta x_n^0 = v_n T + D$ – as in Eq. (2) – with the parameters values $T = 1$ and $D = 1$. The reason is that in the deterministic NS model $a_{(1)}(\Delta x_n) = 0$ for $\Delta x_n = v_n$, implying that this is the optimal headway Δx_n^0. To obtain the function $a_{(1)}(\Delta x_n)$ we recall that in the NS model the acceleration a_n is equal to 1 for $\Delta x_n > \Delta x_n^0$, and that the velocity is reduced to $\Delta x_n - 1$ for $\Delta x_n > \Delta x_n^0$. Therefore

$$a_{(1)}(\Delta x_n) = \begin{cases} 1, & \Delta x_n \geq \Delta x_n^0 \\ \\ \Delta x_n - \Delta x_n^0, & \Delta x_n \geq \Delta x_n^0. \end{cases} \tag{8}$$

for the deterministic NS model ($p = 0$). The plot of this piecewise linear discrete function is displayed in Fig. 1b in circles, and can be compared to $a_{(1)}(\Delta x_n)$ of our model (thin curve).

For the stochastic NS model ($0 < p < 1$), a function $a_{(1)}(\Delta x_n)$ can represent the average behavior of cars. Therefore $a_{(1)}$ can be found here by subtracting p from the deterministic $a_{(1)}$ in Eq. (8), according to the randomness rule in the NS model [15]. Therefore $a_{(1)}(\Delta x_n)$ remains a piecewise linear function also for the stochastic NS model (Fig. 1b, squares). Note that in both the deterministic and

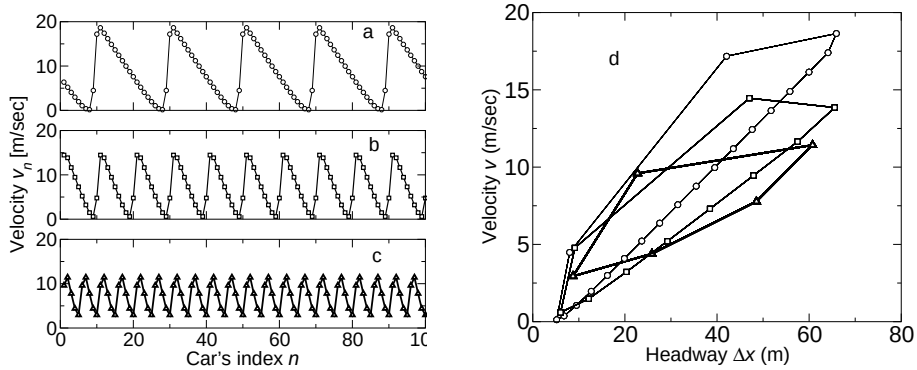

Fig. 2. Three different stable stop-and-go states of the same density $\rho = 0.03veh/m$, $A = 1m/s^2$, and $v_{per} = 25m/s$. Figs. a-c presents the velocities of all cars of these states, which also yield different values of flux f. **a.** $\lambda = 20veh$ ($f = 0.2618veh/sec$), **b.** $\lambda = 10veh$ ($f = 0.2160veh/sec$), and **c.** $\lambda = 5veh$ ($f = 0.2168veh/sec$). **d.** Headway-velocity diagrams of the three limit cycles in Figs. a-c: $\lambda = 20veh$ (circles), $\lambda = 10veh$ (quares), and $\lambda = 5veh$ (triangles).

the stochastic NS models, $a_{(1)}(\Delta x_n)$ becomes a linear function for $v_n = v_{max}$. In this case the horizontal part of $a_{(1)}(\Delta x_n)$ can be replaced with any positive function, due to the influence of the maximal velocity term $a_{(3)}$.

For the stochastic Nagel-Paczuski (NP) model [17], however, random braking can occur only after braking due to insufficient headway. The corresponding function $a_{(1)}(\Delta x_n)$ is therefore a combination of the deterministic NS function (8) for $\Delta x_n < \Delta x_n^0$ and that of the stochastic NS model for $\Delta x_n \geq \Delta x_n^0$ (see Fig. 1b, dashed curve with full symbols). Note that unlike the NS models [15,16], both the NP and our model demonstrate metastable free flow (see [17,11]). Note also that unlike the NS models in which $a_{(1)}(\Delta x_n)$ is linear for stable free flow, this function is not linear for both NP model and our model. This additional nonlinearity seems to be essential for the existence of bistable regime.

3 The Generalized Fundamental Diagram

The solutions of the deterministic model Eq. (7) for the intermediate density regime are characterized by periodic density waves. Simulations of our model show the existence of multiple stable states which correspond to limit cycles in the phase space. Figs. 2a-c present the velocities of all cars on a road after sufficient relaxation time, for three different initial conditions. It can be seen that the wavelengths λ of these states (in the vehicle space) is different. Note that the flux of these states has also different values (see caption of Fig. 2).

Our numerical simulations also show the existence of other solutions with other wavelengths and flux values than that displayed in Fig. 2a-c. Consequently, depending on initial conditions, different stable wave solutions can emerge with

different distances between neighboring humps and different values of flux. This indicates that for intermediate values of densities system (7) has many stable periodic (in, e.g., $\Delta x_n, \Delta v_n$ variables) solutions. Hence, in the $2N$-dimensional space of variables $\Delta x_n, \Delta v_n$ there exist many attractive limit cycles. Three examples of these limit cycles are presented in Fig. 2d, for the same states presented in Figs. 2a-c.

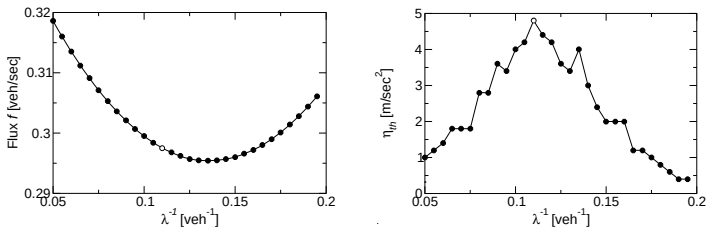

Fig. 3. **a**. Typical dependence of the flux on the wavelength. The global density is $\rho = 0.06veh/m$, $A = 3m/s^2$, and $v_{per} = 25m/s$. **b**. Noise stability threshold of the stable states displayed in the previous Figure, as a function of the wavelength.

As implied above, the flux for the limit cycles is not only a function of the density, but also depends on the wavelength. A typical relation between the flux and the wavelength for some given density is shown in Fig. 3a. As can be seen in this figure, the flux-wavelength relation usually has a single minimum.

Fig. 3a also indicates that similarly to Kerners' empirical findings, here also there exist a range of possible stable flux values for some given value of density. Note that the stable periodic states of the OVM [13] are having the same value of flux for a given density ($f = f(\rho)$ but $f \neq f(\lambda)$, see [14]). The same holds for the deterministic NS model [15], where for all stable states f depends on ρ only. For our model, however, the flux is not only a function of the density, but also of the wavelength of stop-and-go traffic waves,

$$f = f(\rho, \lambda). \tag{9}$$

Thus, the fundamental diagram (flux-density relation) has to be generalized into the *generalized fundamental diagram* (GFD) – a flux-density-wavelength relation.

To obtain this flux-density-wavelength relation we perform extensive simulations of the deterministic model Eq. (7) on homogeneous systems with periodic boundary conditions, starting from different initial conditions [27]. In these simulations, the density of cars can easily be controlled, due to conservation of mass. However, controlling the wavelength is more difficult. For this purpose it is necessary to start with periodic initial conditions, such as equal initial spacing between cars and harmonic dependence of the initial velocity on the cars indexes. But even this consideration may not be enough, since in the basin of attraction of a limit cycle with some wavelength λ does not necessarily include the corresponding harmonic initial states. To overcome this difficulty, we also

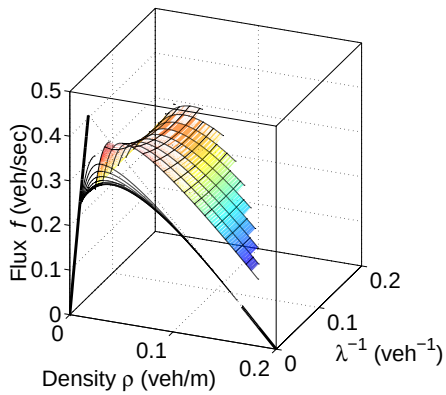

Fig. 4. The generalized fundamental diagram (GFD) – flux-density-wavelength relation for the different states of the deterministic model: stable stop-and-go states (surface), stable and unstable homogeneous states (thick and dotted lines, respectively). The wavelength is defined as the average distance (in the vehicles space) between centers of two nearest dense regions in stop-and-go traffic. Some curves with fixed wavelength ($\lambda = 2/60, 3/60, \ldots, 12/60$) are projected on the density-flux plane (thin curves). The cross-section of the surface for a density constant density $\rho = 0.06 veh/m$ is shown in Fig. 3a, demonstrating the typical dependence of the flux on the wavelength.

use as initial conditions the steady state of some other density with the same wavelength, which are rescaled in order to obtain the desired density.

As a result we derive the generalized fundamental diagram (flux-density-wavelength relation) shown in Fig. 4. This figure presents the flux measured for the steady states of the deterministic model: stop-and-go waves (surface), homogeneous free and homogeneous congested flow (thick lines). The projection of the surface in Fig. 4 on the density-flux plane (thin curves in Fig. 4) provides a two-dimensional region of stable states, qualitatively similar to that found empirically [7,8] for synchronized flow. Note that this result is obtained even for a deterministic model. Thus, in contrast to the common belief that the flux depends only on the density of cars (fundamental diagram), we obtain a generalized fundamental diagram (Fig. 4) which shows that the flux depends on two variables – density ρ and wavelength λ.

4 The Influence of Noise

In the previous section we have studied the deterministic version of our model, with zero noise term in Eq. (7). Nevertheless, real traffic is characterized by the presence of noise, mainly caused by some randomness in the behavior of each single driver, which is our concern in this Section. Our simulations show that even for non-zero noise amplitude, the stop-and-go waves remain stable until some threshold amplitude is reached. But some of the limit cycles are more

sensitive to noise than others. For sufficiently large noise amplitude η, the system moves from these metastable states to more stable states. An example for such transition was demonstrated in [11].

To determine the threshold amplitude of noise, extensive simulations have been performed, starting from various initial limit cycles. In these simulations the noise amplitude has been gradually increased, starting from $\eta = 0$. Every increase of the noise was followed by sufficiently large transient and evaluation time, during which the average wavelength has been evaluated. The evaluation of the wavelength has been performed directly by measuring all velocities, $v(n)$, and counting the number of times this function crosses the average velocity v. The criterion for supercritical noise (or loss of stability) is the presence of wavelength which different from the initial wavelength for more than 50% of the evaluation period. Using this technique, the noise stability threshold η_{th} is evaluated for different values of wavelength. A typical relation between η_{th} and λ is shown in Fig. 3b, for $\rho = 0.06$. This figure can be compared to Fig. 3a, where the same parameters have been used, and the flux of the same states is shown.

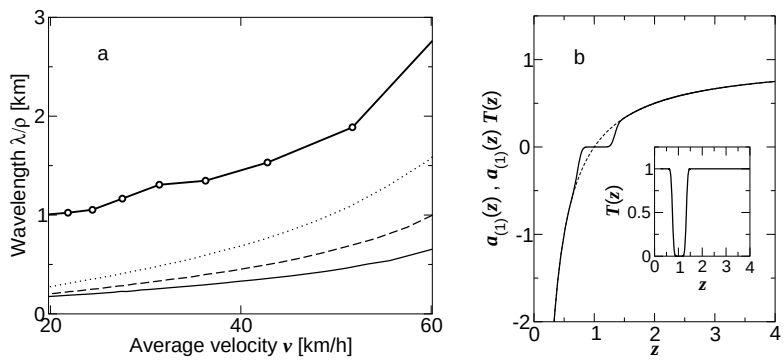

Fig. 5. a. The average wavelength of the stop-and-go states (in real space) as a function of the average velocity. Random initial conditions were applied for different values of density, and the λ and v were measured after sufficiently long transient time, and averaged many iterations of each density. This relation is displayed for the common model, Eq. (7), with $A = 3m/sec^2$ (solid lower curve), $A = 1.5m/sec^2$ (dashed curve), $A = 0.75m/sec^2$ (dotted curve), and for the threshold version of the model with $A = 3m/sec^2$ (solid upper curve). **b**. The threshold version of the model. The solid curve corresponds to the modified function $a_{(1)}$ which includes the threshold in the reaction of the driver, given by Eq. (11), $A = 1m/sec^2$. It can be compared to the unmodified expression (dashed curve) with the same value of A. The threshold function (10) is displayed in the inset.

As can be seen in Fig. 3b, intermediate values of wavelengths are the most stable in the presence of noise. In contrast, cycles with relatively small and relatively large wavelengths are more sensitive to noise, and can be considered as metastable states. The practical meaning of this finding is that for a given

level of noise (below the maximal threshold) only the intermediate part of the possible range of wavelength can be found, and the most probable state is the state with the highest value of threshold. This might be the reason to the fact that in real stop-and-go traffic there exists a typical value of wavelength [7] (see also Sec. 5 below).

From Figs. 3a-b it follows that the most stable state in the presence of noise, denoted by an open circle, has a relatively low value of flux. This fact is one of the motivations for the optimization strategy developed in Sec. 6. The optimization process, which is based on the flux-wavelength relation demonstrated in Fig. 3a, is explained later using our analysis of the different noise thresholds of the different states presented here (Fig. 3b).

5 The Wavelength of Stop-and-Go Traffic

Stop-and-go traffic is a well-known congested traffic state characterized by periodic density waves. This state is characterized by the existence of a characteristic time period (approximately 10 minutes, see [10] and references therein). Recently, the existence of a characteristic lengthscale, which is a function of the average velocity, was also measured for stop-and-go traffic [7]. This wavelength, called 'R_{narrow}', represents the average distance between the narrow jams, and was found to be an increasing function of the average velocity of the synchronized flow downstream.

When comparing the experimental findings to the numerical results of our model, a qualitatively similarity is found. Like the empirical results, the average value of the wavelength (starting from random initial conditions) is found to be an increasing function of the average velocity (see Fig. 5a). However, the values of the wavelength we find are considerably lower than that found by [7]. A better quantitative agreement can be acieved using the threshold version of the model described below.

The existence of threshold level of stimulus required for human response is a well-known phenomenon, which, in our case means that the driver does not accelerate or brake if the headway Δx_n is sufficiently close to the optimal headway Δx_n^0. In other words, drivers usually accelerate (decelerate) only when the difference between the headway and the optimal headway is above (below) some positive (negative) value. The realization of this threshold in our model is by multiplying the acceleration term $a_{(1)}$ given by Eq. (3) with a threshold function, $T(\Delta x_n/\Delta x_n^0) = T(z)$, a function that approaches 0 when $z = \Delta x_n/\Delta x_n^0 \approx 1$, and approaches 1 otherwise. We choose to use the function

$$T(z) = \frac{1}{2}\{1 + erf[\frac{s}{\sqrt{2}}(z - \frac{1}{r})]\frac{1}{2}\{1 + erf[\frac{s}{\sqrt{2}}(r - z)]\}. \tag{10}$$

The values of r and $1/r$ determines the upper and lower cutoff values of z, respectively, and s is the quality factor of the cutoff. Here we use the parameters values $r = 0.75$ and $s = 20$. The plot of the function $T(z)$ is displayed in the

inset of Fig. 5b. The obtained threshold acceleration term

$$a_{(1)}(\Delta x_n) = A\left(1 - \frac{\Delta x_n^0}{\Delta x_n}\right) T(\Delta x_n/\Delta x_n^0), \tag{11}$$

is displayed in Fig. 5b, for $A = 1$.

As a result of this modification, the effective A can be close to zero (below the threshold) or close to A (above the threshold). Hence the values of the wavelength are expected to grow. As can be seen from Fig. 5a, the average wavelength (red curve) is close to that measured by Kerner in real stop-and-go traffic (see [7]).

6 Optimization of Congested Traffic by Wavelength Control

Optimization and control of traffic flow [4,28–33] are usually performed using the concept of fundamental diagram of traffic flow (flux-density relation) [4–6]. However, recent experimental studies of Kerner [7,8], indicate that such fundamental diagram does not exist, and that stable synchronized traffic states display a $2D$ region in the density-flux plane. In Sec. 3 we suggest a possible explanation to this finding using the GFD, showing that for a given value of density, there exist a range of possible flux values representing stable states of different wavelengths.

This new theoretical insight will be applied here, in order to achieve the highest possible flux during congestion. For this purpose, a new strategy of optimization is proposed here. The strategy is based on inducing stop-and-go waves on the main road and controlling their wavelength. Using numerical simulations of our stochastic car-following model (7) we show below that this strategy yields optimization of traffic flow when implemented in systems with a localized periodic inhomogeneity.

In the following, two types of systems with a localized periodic inhomogeneity are considered: (a) signalized intersections, and (b) entry ramps with signalized entrances. We focus on cases of over-saturation, i.e., where traffic is congested upstream of the inhomogeneities.

(a) Signalized intersection: Signal optimization theories [4,28–30,32,34] are traditionally concerned with optimizing global quantities such as the total delay time of all drivers in the system. Our aim here is different – to optimize the flux in an arbitrary direction of an intersection. In an oversaturated signalized intersection, however, the flux in each direction upstream to the intersection is influenced only by the parameters of the traffic signals of this direction. Thus we can consider a single direction for simplicity (as, e.g., in [28]).

In the studied system, traffic lights are placed at position $L/2$ on a road with length L and periodic boundary conditions. The flux f is measured at the position of the traffic lights. We assume that during a given portion P_r of the total signal periods τ, the intersection is occupied by vehicles coming from the other directions. The rest of the time in each signal period is divided into three parts: τ_g and τ_y are the durations of the green and yellow [36] lights, and τ_- is a given additional safety red light period. Thus $\tau = P_r\tau + \tau_g + \tau_y + \tau_-$.

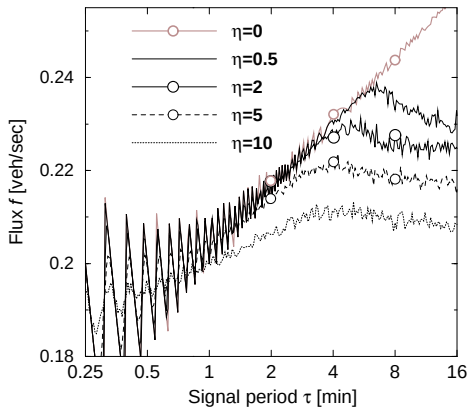

Fig. 6. Relation between signal period and flux for the values of acceleration noise amplitude $\eta = 0, 0.5, 2, 5, 10 m/sec^2$ (top to bottom). Traffic lights parameters are $P_r = 1/3$, $\tau_y = \tau_- = 2sec$. The total number of cars in the system is $N = 400$ and its length is $L = 10km$. While according to Eq. (12) almost no influence of τ on f is expected, the numerical simulations of the deterministic model ($\eta = 0$, upper curve) show that f significantly increases with τ even for large values of τ. Moreover, an optimal signal period is found when the stochastic model is used ($\eta > 0$ curves). The nine open circles correspond to the nine instances shown in Fig. 7.

The period of yellow light is realized as follows. When the light is changed from green to yellow, all simulated drivers upstream of the intersection estimate the intersection crossing time t_n by a linear extrapolation of their position. The first car that begins to stop, s, is the first car that is not able to cross before the light changes to red, i.e., $t_s = \min\{t_n | t_n > \tau_y\}$). For this car, Δx in Eq. (7) is replaced with the distance between s and the traffic lights. The consecutive cars follow s and stop according to Eq. (7). Due to this procedure cars can still cross the intersection during time τ_y.

As mentioned above, our aim here is to optimize the flux in a single direction of the intersection, without affecting the parameters of the whole complex system of roads. Thus we consider P_r to be a given constraint, and explore the relation between the flux f and the signal period τ. According to common optimization theories, the result is expected to be [28]

$$f = f_0 \left(1 - P_r - \frac{\tau_-}{\tau}\right), \tag{12}$$

where f_0 is the constant flux during the green light period. Eq. (12) simply expresses the fact that the outflow of a single direction is a product of the actual relative green light period and f_0. Since usually $\tau \gg \tau_-$, the flux should be hardly influenced by τ.

However, the results of our simulations are different from Eq. (12) for both stochastic and deterministic models. The typical relation between f and τ for a given density shown in Fig. 6 shows a much greater influence of τ on f than that

predicted by Eq. (12). Apart from trivial flux oscillations which are explained below, Fig. 6 demonstrates a monotonic asimptotic increase of the flux f as τ grows for the deterministic model $\eta = 0$. For the stochastic model $\eta > 0$, however, an optimal signal period can be clearly seen. In this case, a crossover is observed from the deterministic monotonically increasing $f(\tau)$ to a saturated lower value of the flux for large τ. Therefore there exists an optimal signal period that yields maximal flux. Such influence of τ on f is not explained by Eq. (12).

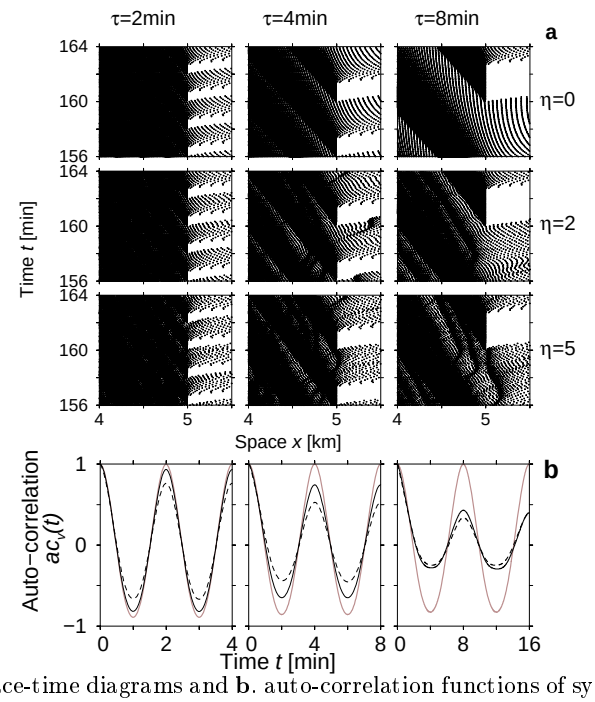

Fig. 7. **a**. Space-time diagrams and **b**. auto-correlation functions of systems with single traffic light with parameters values that are similar to that of the nine instances denoted by circles in Fig. 6. The position of the traffic light is $x = 5km$. The major dense (black) regions moving upstream in Fig. a. are caused by the red light, and the distance between such nearest two regions (corresponding to the wavelength) is growing as τ grows. The grey curves in Fig. b. correspond to $\eta = 0$, the solid curves to $\eta = 2$, and the dashed curves to $\eta = 5$. Comparison to Fig. 6 indicates that the crossover to reduced values of flux in the latter Figure is related to the emergence of small jams, which causes loss of the periodicity (see Fig. a) as well as reduced values of the auto-correlation function, $ac_v(t = \tau)$ (see Fig. b.)

In contrast to [30], where the oscillations observed in $f(\tau)$ have been related to degree of synchronization of the green lights in the network, here the oscillations are a trivial result of the discrete nature of the flowing media. Since all vehicles have the same parameters, the crossing times of the intersection is identical in each period. This causes discretization in the average number of crossing cars in each period, n, which becomes a staircase function of τ. The flux is given

by $f = n(\tau)/\tau$, and hence the magnitude of these oscillations decreases with increasing τ.

The existence of an optimal signal period can now be explained using our finding of the influence of λ on the flux and on η_{th}. First, it is easy to see that the signal period τ controls the wavelength λ of stable stop-and-go waves that are induced by the traffic lights, as $\lambda = v\tau$, where v is the wave velocity [6]. From Fig. 3a it appears that in order to increase the flux, λ – and therefore τ – should be increased [37]. For this reason the deterministic model yields a monotonically increasing $f(\tau)$ (Fig. 6, upper curve). However, for the stochastic model ($\eta > 0$), states for which $\eta_{th}(\lambda) < \eta$ become unstable according to Fig. 3b – in particular those with relatively high values of λ, which in principle should yield higher values of flux. The increase of the flux with increasing τ thus crosses-over to lower values due to the instability of the induced waves. The existence of an optimal τ is a result of this effect.

We can therefore see that the non-trivial flux-wavelength relation is the reason for the unexpected behavior of $f(\tau)$. The deviations between the theoretical prediction of Eq. (12) and the numerical measurements of the deterministic model (Fig. 6) can be explained using the GFD. The crossover in $f(\tau)$ for the stochastic model, and the existence of an optimal τ are related to the loss of the stability of the states with relatively large wavelength due to the noise. Eq. (12) can be now modified by assigning $f_0 = f_0(\tau, \eta)$.

To obtain further support of this explanation let us evaluate a measure for the periodicity of the flow using single vehicle data collected at the intersection. We calculate the auto-correlation function $ac_v(t)$ [10] of the velocity function $v(t')$ measured at the intersection,

$$ac_v(t) = \frac{< v(t')v(t'+t) > - < v(t') >< v(t'+t) >}{< v(t')^2 > - < v(t') >^2}, \tag{13}$$

where a linear interpolation of the discrete function $v(t)$ is used. The brackets $< \ldots >$ indicate averaging over time t'. Displayed in Fig. 7b are the auto-correlation functions for the nine instances of Fig. 7a, respectively. As can be seen from this Figure, $ac_v(t = \tau) = 1$ for all the $\eta = 0$ instances, implying that the flow for these cases is completely periodic, and that the time period of $v(t)$ is exactly τ. A comparison of all instances shown in Fig. 7b to the data in Fig. 6 shows that the flux approaches the deterministic value as long as $ac_v(t = \tau) \approx 1$. As η or τ are increased, the flow is no longer periodic ($ac_v(t = \tau) < 1$ in Fig. 7b), small jams emerge (Fig. 7a), and the flux becomes lower (Fig. 6).

(b) Entry ramp with signalized entrance: It is a well-know fact that congestion often occurs upstream to entry ramps [9,11,24–26]. A common way to relieve congestions in this case is to control the entrances by traffic signals. The idea is to prevent congestion by homogenizing the flow – by letting cars enter only into low-density regions. Clearly, this method is more efficient for intermediate densities rather than for high densities where congestion cannot be avoided. In the following we examine the possibility of optimization of such congested systems. The traffic light will be used to induce stable stop-and-go waves with optimal wavelength on the main congested road.

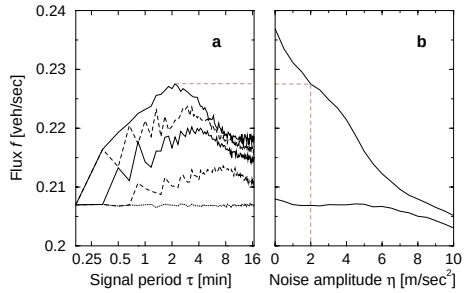

Fig. 8. (a) Relation between signal period on the entry ramp and flux on the main road, for $P_r = 0.7, 0.5, 0.4, 0.2, 0.0$ (top to bottom), and for noise amplitude $\eta = 2m/s^2$. The total number of cars in the system is $N = 300$, the system length is $L = 10km$, and the flux is locally measured on the main road at $100m$ upstream to the on-ramp. Here $f_{in} = 0.1veh/s$ and $f_{max} = 0.333veh/s$. (b) A comparison between the optimal flux (upper curve) and the flux without the presence of a traffic light (lower curve), as a function of η.

The system studied here has periodic boundary conditions and a single entry ramp [33,34]. To make this inhomogeneity periodic, we introduce traffic signals at the downstream end of the entry ramp, and study its effect on the flux on the main road. The incoming vehicles are allowed to enter the main road during the green light period τ_g, and are delayed during the red light period $P_r\tau$, so here $\tau = P_r\tau + \tau_g$. Unlike the signalized intersection where P_r was predetermined, here it is one of the optimization parameters, in addition to τ. Similar to [24], we introduce an exit ramp at a large distance from the entry ramp, so that the total number of cars in the system is conserved. The entrance and the exit of cars from the ramps are performed in the same manner as in [11]. We focus on cases where the average flux of the incoming vehicles f_{in} causes congestion on the main road (see [9,25]), but the secondary road is not congested. Since our goal is to optimize the flux on the main road without causing congestion on the secondary road, we set an upper bound for P_r. This bound is $P_r \leq 1 - f_{in}/f_{max}$, where f_{max} is the maximal possible value of the incoming flux, since cars approach the queue upstream to the traffic light with rate f_{in}, and this queue is discharged with rate f_{max} during the green light.

Typical relations between flux and signal period are plotted in Fig. 8a, for different values of P_r and for $\eta = 2m/s^2$. Note that the curve corresponding to an unsignalized entry ramp ($P_r = 0$) is the lowest, implying that the introduction of a traffic light increases the flux on the main road. Moreover, the increase in the flux on the main road is obtained without causing congestion on the secondary road, as we consider only the values of P_r which are below this congestion threshold. The relative increase in the flux due to the introduction of a traffic light with optimal parameters (Fig. 8b) varies from 1.0% for $\eta = 10m/s^2$, through 10.0% for $\eta = 2m/s^2$ and up to 13.9% for $\eta = 0$. This increase of the flux f has even a more significant influence on the growth rate of the congested

section of highway upstream of the entry ramp, since this rate is proportional [6] to $f' - f$, where f' is the flux upstream to this region. These results suggest that even when congestion of real traffic cannot be relieved, the flux can be increased by an optimal signalization of entry ramps to control and stabilize stop-and-go waves.

In addition to the two studied systems, the new optimization approach may also be efficient in traffic control systems that are based on varying speed limits along the road. In these systems, stop-and-go traffic waves can be controlled [35], and therefore can also be optimized using this approach.

To summarize, this work was motivated by the new experimental findings of a two-dimensional representation of synchronized flow in the density-flux plane [7,8]. Using a deterministic car following model [11] we are able to show that the fundamental diagram has to be generalized to include another variable, the wavelength of the stop-and-go waves. The projection of the generalized fundamental diagram (GFD) on the density-flux plane yields a two-dimensional region of stable states, qualitatively similar to that found experimentally for synchronized flow. The different states also differ in their sensitivity to noise. The dependence of the wavelength of the most attractive state on the average velocity is qualitatively similar to that found experimentally. Quantitative agreement can be also approached by including threshold in the driver's reaction. We use these theoretical predictions to propose a novel strategy for traffic optimization, based on inducing stable stop-and-go waves yielding the maximal flux. In general, the interplay between the wavelength-flux relation (Fig. 3a) and the noise stability threshold of the different states (Fig. 3b) determines the optimal wavelength and signal period.

Nevertheless, the encouraging results obtained for the studied systems are mostly based on numerical simulations and analytical studies. A careful field study is thus necessary to verify the model predictions, especially the generalized fundamental diagram, and to test the optimization mechanism.

References

1. D. Chowdhury, L. Santen, A. Schadschneider: Phys. Rep. **329**, 199 (2000)
2. D. Helbing: Rev. Mod. Phys. (in the press) (2001); cond-mat/0012229 (2000)
3. D.E. Wolf: Physica A **263**, 438 (1999)
4. A.D. May: *Traffic Flow Fundamentals*, (Prentice Hall, Englewood Cliffs, N.J. 1990)
5. B.D. Greenshields: High. Res. Rec. **14** 468 (1934)
6. M.J. Lighthill G.B. Whitham: Proc. R. Soc. London Ser. A **229**, 317, (1955)
7. B.S. Kerner: Phys. Rev. Lett. **81**, 3797 (1998)
8. B.S. Kerner: Physics World **12** (8), 25 (1999)
9. B.S. Kerner, H. Rehborn: Phys. Rev. Lett. **79**, 4030 (1997)
10. L. Neubert, L. Santen, A. Schadschneider, M. Schreckenberg: Phys. Rev. E **60**, 6480 (1999)
11. E. Tomer, L. Safonov, S. Havlin: Phys. Rev. Lett. **84**, 382 (2000)
12. L.A. Safonov, E. Tomer, V.V. Strygin, S. Havlin: Physica A **285**, 147 (2000)
13. M. Bando, K. Hasebe, A. Nakayama, A. Shibata Y. Sugiyama: Phys. Rev. E **51**, 1035 (1995)

14. Y. Sugiyama: 'Dynamical Model for Congestion of Freeway Traffic and its Stractural Stability'. In: *Traffic and Granular Flow*, ed. by D.E. Wolf, M. Schreckenberg, A. Bachem (World Scientific, Singapore 1996) pp 137–149
15. K. Nagel, M. Schreckenberg, J. Phys. I (France) **2**, 2221 (1992)
16. K. Nagel, H.J. Herrmann: Physica A **199**, 254 (1993)
17. K. Nagel, M. Paczuski: Phys. Rev. E **51**, 2909 (1995)
18. O. Biham, A.A. Middleton, D. Levine: Phys. Rev. A. **46**, R6124-R6127 (1992)
19. R. Herman, R.W. Rothery: 'Car Following and Steady State Flow'. In: *Proceedings of the 2ns International Symposium on the Theory of Road Traffic Flow, London, 1963*, ed. by J. Almond, (Organization for Economic Cooperation and Development, Paris 1965) pp 1–11
20. D. Helbing, B. Tilch: Phys. Rev. E **58**, 133 (1998)
21. N. Mitarai, H. Nakanishi: Phys. Rev. Lett. **85**, 1766 (2000)
22. M. Treiber, A. Hennecke, D. Helbing: Phys. Rev. E **62**, 1805 (2000)
23. S. Cheybani, J. Kertesz, M. Schreckenberg: Phys. Rev. E. **63**, 016108 (2001)
24. H.Y. Lee, H.W. Lee, D. Kim: Phys. Rev. Lett. **81**, 1130 (1998)
25. D. Helbing, M. Treiber: Science **282**, 2001 (1998)
26. D. Helbing, A. Hennecke, M. Treiber: Phys. Rev. Lett. **82**, 4360 (1999)
27. Interactive simulations of the deterministic model with and without traffic lights can be found at http://ory.ph.biu.ac.il/2000/traffic/
28. D.C. Gazis, R.B. Potts: 'The Over-Saturated Intersection'. In: *Proceedings of the 2ns International Symposium on the Theory of Road Traffic Flow, London, 1963*, ed. by J. Almond, (Organization for Economic Cooperation and Development, Paris 1965) pp 221–237
29. W.B. Cronje: Transport. Res. Rec. **905**, 80 (1983)
30. D. Chowdhury, A. Schadschneider: Phys. Rev. E. **59**, R1311 (1999)
31. N. H. Gartner, C. Stamatiadis, and P. J. Tarnoff, Transport. Res. Rec. **1494**, 98 (1995)
32. T.H. Chang, J.T. Lin, Transport. Res. B **34**, 471 (2000)
33. H. Zhang, S.G. Ritchie, W.W. Recker: Transport. Res. C **4**, 51 (1996)
34. M. Treiber, D. Helbing, *preprint* (2001)
35. R. Sollacher, H. Lenz: 'Nonlinear Control of Stop-and-Go Traffic'. In: *Traffic and Granular Flow '99*, ed. by D. Helbing, H.J. Herrmann, M. Schreckenberg, D.E. Wolf, (Springer, Berlin 2000) pp 315–320
36. The period of yellow light is realized as follows. When the light is changed from green to yellow, all simulated drivers upstream to the intersection estimate the intersection crossing time t_n by a linear extrapolation of their position. The first car that begins to stop, s, is the first car that is not able to cross before the light changes to red, i.e., $t_s = min\{t_n | t_n > \tau_y\}$). For this car, Δx in Eq. (7) is replaced with the distance between s and the traffic lights. The consecutive cars follow s and stop according to Eq. (7). Due to this procedure cars can still cross the intersection during time τ_y.
37. Decreasing λ and τ would not yield the same result due to relatively large values of τ_-/τ in Eq. (12).